Journal of Colloid and Interface Science 356 (2011) 257–261

Contents lists available at ScienceDirect

Journal of Colloid and Interface Science

www.elsevier.com/locate/jcis

Photocatalytic reduction of CO_2 in methanol to methyl formate over CuO–TiO_2 composite catalysts

Shiyue Qin [a], Feng Xin [a,*], Yuande Liu [a], Xiaohong Yin [b], Wei Ma [b]

[a] School of Chemical Engineering and Technology, Tianjin University, Tianjin 300072, China
[b] School of Chemistry and Chemical Engineering, Tianjin University of Technology, Tianjin 300384, China

ARTICLE INFO

Article history:
Received 15 October 2010
Accepted 7 December 2010
Available online 15 December 2010

Keywords:
Photocatalysis
Photocatalytic reduction of CO_2
Composite semiconductor
Methanol
Methyl formate

ABSTRACT

Photocatalytic reduction of CO_2 on CuO–TiO_2 composite catalysts in the presence of methanol to prepare methyl formate had been investigated. Methanol was used as sacrificial reagent to react with the photogenerated holes in the valence band, and CO_2 was reduced by the electrons in the conduction band. CuO–TiO_2 was optimized for CuO loading, preparation method and calcination temperature. The catalyst of 1.0CuO–TiO_2, calcined at 450 °C and CTAB as a dispersant showed the highest overall activity. The heterojunction between CuO and TiO_2 demonstrated with HRTEM played an important role in enhancing the photocatalytic activity.

© 2010 Elsevier Inc. All rights reserved.

1. Introduction

The rapid increase in atmospheric CO_2 leads to climate change, which is one of the greatest threats of times. It is urgent to reduce the accumulation of CO_2 in the atmosphere. There are three ways to reduce CO_2 emissions: reducing the amount of the produced CO_2, using CO_2 and storing CO_2, where transformation of CO_2 into chemicals is an attractive option and fulfills the recycle use of CO_2.

Photoreduction of CO_2 is a possible avenue to convert CO_2. In 1979 Honda et al. first reported photoreduction of CO_2 to organic compound such as HCOOH, HCHO, CH_3OH and CH_4 in aqueous suspension of semiconductor powders [1]. A number of researches focused on the photocatalytic reduction of CO_2 with H_2O [2–8]. Because of the weak reducibility of water and the low solubility of CO_2 in water, many other reductants were used for the photoreduction of CO_2. Teramura et al. used Ga_2O_3 as a photocatalyst for the photocatalytic reduction of CO_2 in the presence of H_2 which worked as a reductant and CO gas was selectively produced [9]. Lo et al. studied photocatalytic reduction of CO_2 in a self-designed circulated photocatalytic reaction system under TiO_2 and ZrO_2 photocatalysts and the highest yield of the photoreduction of CO_2 was obtained by using TiO_2 with $H_2 + H_2O$ and ZrO_2 with H_2 [10]. Teramura et al. used MgO for photoreducing CO_2 to CO in the presence of H_2 or CH_4 and clarified the mechanism of the CO_2 photocatalytic reduction [11]. Al-Jubori described the photoelectrocatalytic reduction of carbon dioxide in aqueous solution to C1 organic compounds (formic acid and formaldehyde) in the presence of n-Bi_2S_3 and n-CdS semiconductor powders and hydrogen sulfide could enhance the rate of the photoreduction processes [12].

Due to the low rate of photocatalytic CO_2 conversion, following strategies had been employed to enhance photocatalytic carbon dioxide disappearance rate in this paper: (i) use cetyltrimethylammonium bromide (CTAB) as a dispersant to synthesized nanocatalysts with suitable particle size; (ii) CuO and TiO_2 formed composite or heterojunction to reduce the recombination of the electrons and holes; (iii) methanol was used as reductant for the photoreduction of CO_2 because of the stronger reducibility of methanol and solubility of CO_2 in methanol.

2. Materials and methods

2.1. Preparation of catalysts

All the reagents were of analytical purity and purchased from Tianjin Benchmark Chemical Reagent Company. TBOT (tetrabutyl titanate) and CTAB were dissolved in absolute ethanol by sonicating for 15 min and followed by stirring for 15 min respectively. The two solutions were mixed under stirring for 30 min to form a transparent solution. $Cu(NO_3)_2$ $5H_2O$ was dissolved under stirring in absolute ethanol, then the solution of $Cu(NO_3)_2$ was added dropwise to the TBOT + CTAB solution. After stirring for 30 min, the mixture was aged at room temperature for 12 h, then dried at 100 °C overnight. To remove organics, the as-synthesized sample was calcined by temperature program increase of 2 °C/min from room temperature to 450 °C and kept for 6 h. The molar ratio of

* Corresponding author. Fax: +86 22 27892359.
E-mail address: xinf@tju.edu.cn (F. Xin).

0021-9797/$ - see front matter © 2010 Elsevier Inc. All rights reserved.
doi:10.1016/j.jcis.2010.12.034

TBOT + $Cu(NO_3)_2$: CTAB was 1:0.12. The catalysts were assignated as xCuO–TiO_2, where "x" represented the weight percentage of CuO in the catalyst. For comparison, the CuO–TiO_2 samples were also prepared in the above method without adding CTAB or calcinated at different temperatures.

2.2. Characterization of catalysts

The catalysts were investigated by X-ray diffraction (XRD, Bruke/D8-Advance, Cu Kα) at a scan rate of 0.02°s^{-1}. The operation voltage and current were maintained at 40 kV and 40 mA, and the particle size was estimated using the Scherrer equation. The microstructures were observed by a high-resolution transmission electron microscopy (HRTEM: Tecnai G2 F20; accelerating voltage, 200 kV). Light absorbance was measured by UV–vis diffuse reflectance spectroscopy (Shimadzu UV-2550) in wavelength of 190–800 nm by using $BaSO_4$ as a reference.

2.3. Photocatalytic reactions

The photocatalytic reduction of CO_2 under UV light was carried out in a slurry reactor system (Fig. 1). A flat top cover of the vessel was made of Pyrex. The reactor vessel was irradiated, from top of the reactor, by a 250 W high pressure mercury lamp with the radiation peak at about 365 nm. The reaction temperature was 25 ± 3 °C controlled by thermostatic waterbath. Reaction suspension was prepared by using 30 ml of methanol solution and 30 mg of catalyst powders. The reactor was tightly closed during the reaction and a magnetic stirrer agitated the suspension at the bottom to prevent sedimentation of the catalyst. CO_2 (99.99% purity) was bubbled through the reactor at a rate of 100 ml/min for 30 min to purge air and saturate the suspension. The products were qualified by GC–MS (Agilent 5975C) and quantified by GC-FID equipped with HJ.10 capillary column. The activities of different catalysts were compared by the average formation rate of methyl formate (MF) in a period of 6 h. The blank tests consisted of a reaction under light without the catalysts and a reaction in the dark with the catalysts, and there were no products formed.

3. Results and discussion

3.1. Catalysts characterization with XRD, UV–vis and TEM

As shown in Fig. 2, both position and shape of the diffractive peaks of 1.0CuO–TiO_2 were quite similar to pure anatase TiO_2, which indicated that loading small amount of CuO almost did not change the crystalline phase of TiO_2. The diffraction peak of crystal plane [1 0 1] was selected to estimate the crystallite size of the sample by the Debye–Scherrer equation. The mean particle size was nearly 13.8 nm. CuO was not found due to a bit of CuO loading and perfect dispersion.

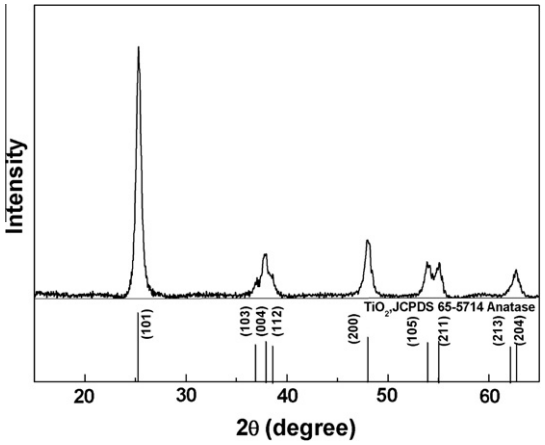

Fig. 2. XRD pattern of 1.0CuO–TiO_2(CTAB, 450 °C).

The 1.0CuO–TiO_2 catalyst was also characterized with TEM and HRTEM to investigate the interfacial structures between CuO and TiO_2. In Fig. 3a, the morphology of particles was uniform and the diameter was about 14 nm, which was consistent with the calculation from XRD pattern. In Fig. 3b the lattice fringes of CuO and TiO_2 clearly showed the surface-phase junction of the composite catalyst. The [1 1 0] lattice fringe of monoclinic CuO was 0.275 nm, and the [1 0 1] lattice fringe of anatase was 0.35 nm [13,14]. The formation of the surface-junction could promote the interparticle charge migration and facilitate the photo-generated electron transfer from conduction band of the TiO_2 to the valence band of CuO (Fig. 8), thereby improving the charge separation efficiency and enhancing the photocatalytic activity.

In Fig. 4, UV–vis DRS spectra revealed that TiO_2 displayed no significant absorbance for visible light due to the large energy gap of TiO_2 (3.2 eV). The CuO–TiO_2 showed spectral response in the visible region (λ = 400–800 nm), and the absorption intensity increased with the increase in the amount of CuO loading in the visible region. In theory, when the absorption intensity increases, the formation rate of electron–hole pairs on the photocatalyst surface also increases, resulting in the photocatalyst exhibiting higher photocatalytic activity.

3.2. The photocatalytic reduction of CO_2

Fig. 5 showed the activities of various catalysts during photocatalytic reduction of CO_2 under irradiation. The catalysts were formed using CTAB as the dispersant and calcined at 450 °C.

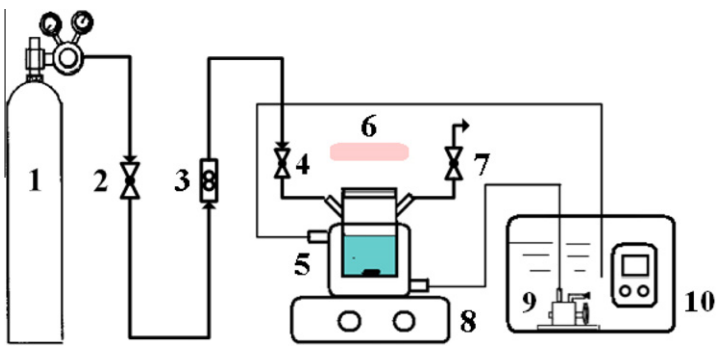

Fig. 1. The scheme of the photocatalytic reaction system: (1) CO_2 steel cylinder, (2) steady flow valve, (3) flowmeter, (4) CO_2 inlet valve, (5) reactor cell, (6) Hg lamp, (7) CO_2 outlet valve, (8) magnetic stirrer, (9) circulating pump, (10) thermostatic waterbath.

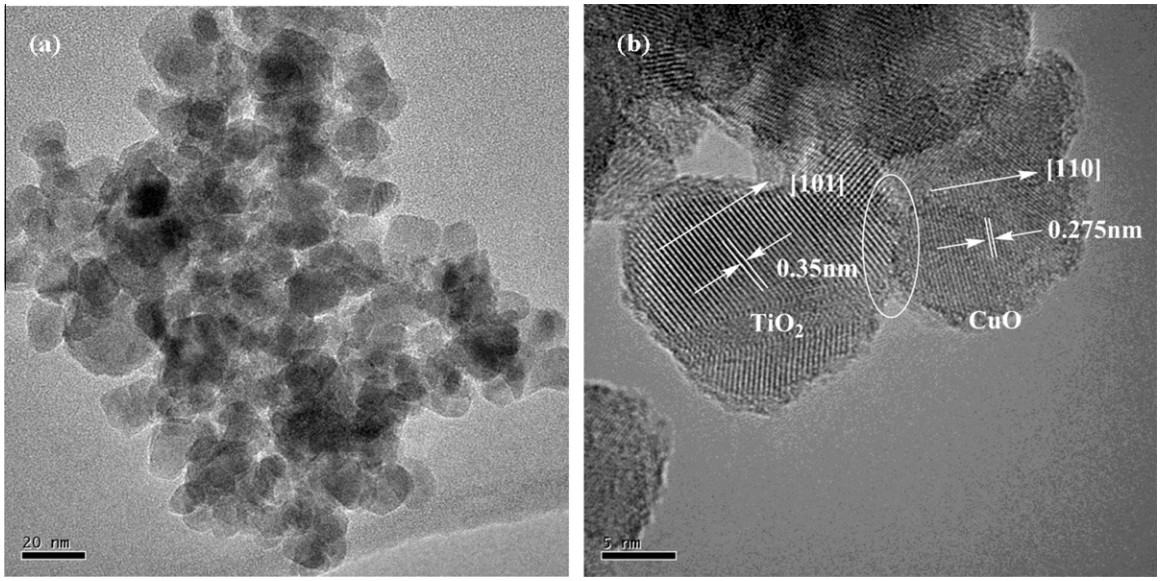

Fig. 3. TEM (a) and HRTEM (b) image of 1.0CuO–TiO_2 (CTAB, 450 °C).

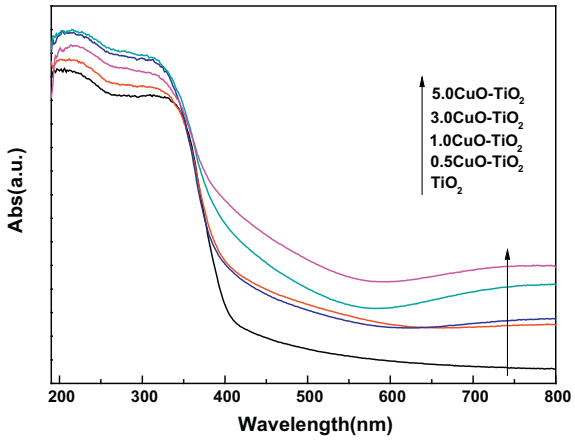

Fig. 4. UV–vis DRS spectra of CuO–TiO_2 (CTAB, 450 °C).

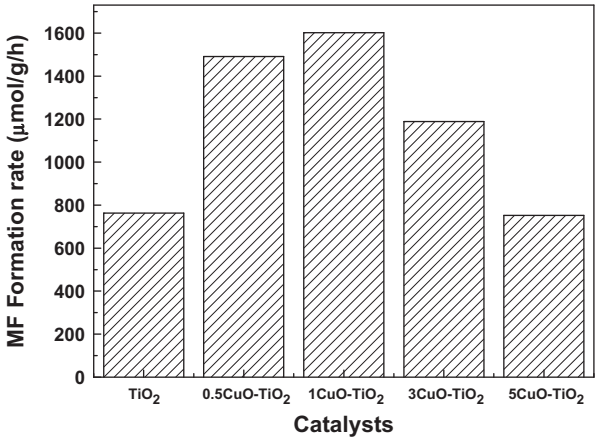

Fig. 5. Formation rate of MF for various catalysts.

Modification of TiO_2 with CuO loading resulted in abrupt increase of the photocatalytic activity because CuO and TiO_2 formed composite catalysts and the recombination of photo-generated electron and hole was restrained. However, higher CuO content (CuO weight percentage >1.0%) was harmful for the activity because of the agglomeration of the CuO particles [15]. It was also seen that the photocatalytic activity was strongly dependent on the amount of CuO loading. The photocatalytic activity increased with the increase in the amount of CuO loading up to 1.0%. When the amount was higher than 1.0%, the photocatalytic activity decreased. From Figs. 4 and 5, we could see that there is no evident relationship between the photocatalytic activity of CuO–TiO_2 and the absorption intensity. Namely, the high absorption intensity did not increase photocatalytic activity in the experimental condition.

From Fig. 6, the CuO–TiO_2 obtained via CTAB exhibited higher activities than the CuO–TiO_2 obtained without CTAB. Since each pair of catalysts exhibited nearly the same crystallinity of anatase at the same calcination temperature, the higher activities of CuO–TiO_2 via CTAB could be attributed to their suitable particle size. The crystallite size plays an important role in nanocrystalline TiO_2 based photocatalysts. Koci et al. prepared pure TiO_2 anatase particles with a crystallite diameters ranging from 4.5 to 29 nm, and the optimum particle size corresponding to the highest yields of products was 14 nm. From Figs. 2 and 3, the mean size of the particle

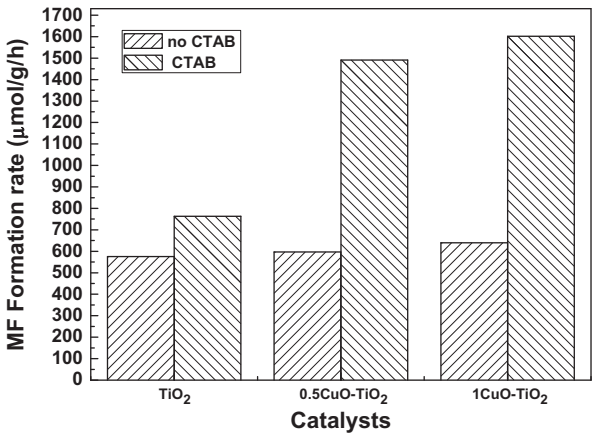

Fig. 6. The effect of preparation method on MF formation rate (450 °C).

was 14 nm, which was close to the optimum size, and the high photocatalytic activity was owing to competing effects of specific surface area, charge-carrier dynamics and light absorption efficiency [3].

Considering the effect of calcination temperature, one could see from Fig. 7 that the 1.0CuO–TiO_2 calcined at 450 °C exhibited higher activity than that calcined at 350 °C and 550 °C. The catalysts were made with CTAB as a dispersant. An important reason was that the 1.0CuO–TiO_2 calcined at 450 °C had better crystallization degree than that calcined at 350 °C [16]. The high crystallinity of anatase facilitated the rapid transfer of photoelectrons from bulk to the surface, and this could effectively inhibit the recombination between photoelectrons and holes, so the quantum efficiency was enhanced [17]. However, calcination of 1.0CuO–TiO_2 at high temperature (550 °C) caused an abrupt decrease in activity because of the sintering of the catalyst.

3.3. The mechanism of the reaction

Fujishima et al. studied electrochemical reduction of CO_2 with high current density in CO_2-methanol medium with changing the pressure of the system from 1 to 60 atm, and CO_2 was reduced to CO, CH_4, C_2H_4, and methyl formate at a Cu electrode [18,19]. Ulagappan et al. studied the photoreduction of gaseous CO_2 in Ti silicalite molecular sieve using methanol as electron donor and the initial products were monitored by in situ FT-IR spectroscopy,

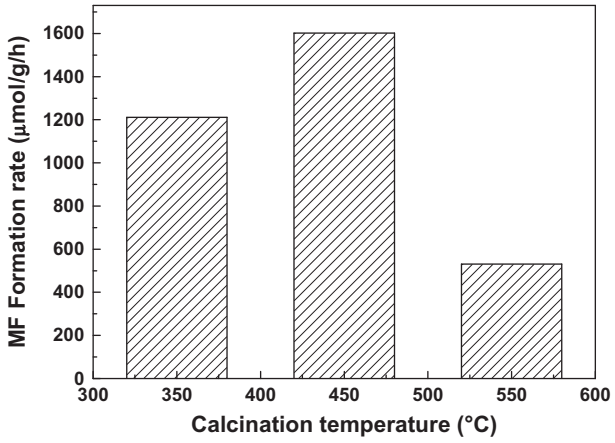

Fig. 7. The effect of calcination temperature on MF formation rate.

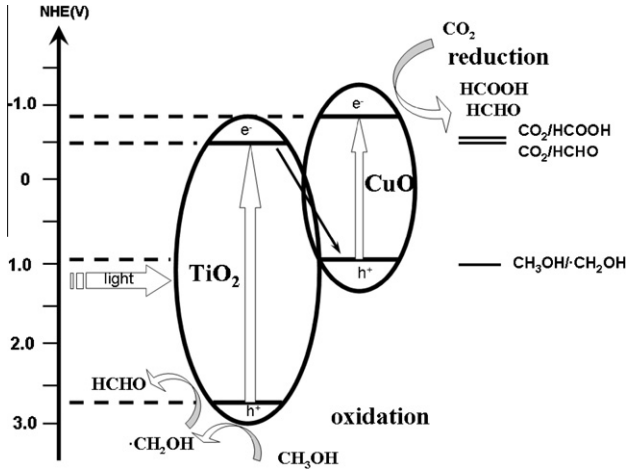

Fig. 8. Band positions of CuO, TiO_2 and the potentials of several redox couples.

where HCOOH, CO, and $HCOOCH_3$ were the observed products [20]. In Fig. 8, CO_2 can be reduced to formic acid and formaldehyde during the photocatalytic reaction. The potential of conduction band of CuO (E_{cb} = −0.78 V) is more negative than those of formic acid and formaldehyde yield, and the potential of valence band of TiO_2 was more positive than those of methanol oxidation [21–23]. The potential of methanol oxidation by a hole to $\cdot CH_2OH$ is $E^0_{CH_3OH/CH_2OH}$ = 0.927 V [24,25]. Methyl formate can be produced through the esterification of formic acid and methanol and dimerization of formaldehyde via Tishchenko reaction [26]. In a comparison experiment, 1.0CuO–TiO_2 was used to investigate the effect of CO_2. In the presence of CO_2, MF formation rate was 1602 μmol/g/h, while in the presence of N_2, MF formation rate was 638 μmol/g/h. If CO_2 was substituted for N_2, methanol was dehydrogenated to $\cdot CH_2OH$and HCHO in the VB and the produced H^+ was reduced to H_2 in the CB. MF was formed through dimerization of formaldehyde but the amount was less than in the presence of CO_2. This suggested that CO_2 was photocatalytic reduced to HCOOH and HCHO and made a main contribution to the formation of MF.

As one of the effective methods for photo-generated electron–hole separation, semiconductor combination is of increasing interest. The method constructs a heterojunction interface between the semiconductors with matching band potentials. Some excited electrons in TiO_2 with a lower CB could recombine with the holes in CuO with a VB close to the CB of TiO_2 (Fig. 8). More powerful excited electrons and holes can be retained on different counterparts. The most obvious merit of these two mechanisms lies in the fact that stronger oxidative holes and reductive electrons can be isolated on TiO_2 and CuO, followed by directly quenching the weaker oxidative holes and reductive electrons in the solid heterostructure intrinsic interfaces.

For efficient carrier separation across the CuO and TiO_2 heterojunction, the CuO should be uniformly distributed and in close/direct contact with the TiO_2 nanoparticles. Fig. 3b showed the HRTEM image of CuO–TiO_2 and demonstrated the heterostructure. In a reference experiment, a mixture of CuO and TiO_2 by mixing with the same ratio as that in the 1.0CuO–TiO_2 heterostructure demonstrated the similar photocatalytic activity as pure TiO_2.

4. Conclusion

The photocatalytic reduction of CO_2 could be enhanced by CuO–TiO_2 composite catalysts by using methanol as sacrificial reagent, and methyl formate was produced. The optimal catalyst was 1.0 wt% CuO loading on TiO_2, CTAB as dispersant, and calcined at 450 °C. The heterojunction between CuO and TiO_2 was found for improving photocatalytic reduction rate of CO_2. The reaction mechanism was also explained by the conventional band theory of charge transfer at the semiconductor materials.

Acknowledgments

We gratefully acknowledge financial support by the National Natural Science Foundation of China (NSFC) 20876109 and 21046006.

References

[1] T. Inoue, A. Fujishima, S. Konishi, K. Honda, Nature 277 (1979) 637.
[2] O.K. Varghese, M. Paulose, T.J. LaTempa, C.A. Grimes, Nano Letters 9 (2009) 731.
[3] K. Koci, L. Obalova, L. Matejova, D. Placha, Z. Lacny, J. Jirkovsky, O. Solcova, Applied Catalysis B-Environmental 89 (2009) 494.
[4] S.S. Tan, L. Zou, E. Hu, Science and Technology of Advanced Materials 8 (2007) 89.
[5] P.W. Pan, Y.W. Chen, Catalysis Communications 8 (2007) 1546.
[6] I.H. Tseng, J.C.S. Wu, H.Y. Chou, Journal of Catalysis 221 (2004) 432.
[7] W.Y. Lin, H. Frei, Journal of the American Chemical Society 127 (2005) 1610.

[8] T. Xie, D. Wang, L. Zhu, T. Li, Y. Xu, Materials Chemistry and Physics 70 (2001) 103.
[9] K. Teramura, H. Tsuneoka, T. Shishido, T. Tanaka, Chemical Physics Letters 467 (2008) 191.
[10] C.C. Lo, C.H. Hung, C.S. Yuan, J.F. Wu, Solar Energy Materials and Solar Cells 91 (2007) 1765.
[11] K. Teramura, T. Tanaka, H. Ishikawa, Y. Kohno, T. Funabiki, Journal of Physical Chemistry B 108 (2004) 346.
[12] S. Aliwi, K. Al-Jubori, Solar Energy Materials 18 (1989) 223.
[13] J. Liu, X. Huang, Y. Li, K. Sulieman, X. He, F. Sun, Crystal Growth and Design 6 (2006) 1690.
[14] J. Zhang, Q. Xu, Z. Feng, M. Li, C. Li, Angewandte Chemie International Edition 47 (2008) 1766.
[15] I. Tseng, Wan-Chen Chang, Jeffrey C.S. Wu, Applied Catalysis B: Environmental 37 (2002) 37.
[16] A.A. Ismail, D.W. Bahnemann, L. Robben, V. Yarovyi, M. Wark, Chemistry of Materials 22 (2010) 108.
[17] M. Hoffmann, S. Martin, W. Choi, D. Bahnemann, Chemical Reviews 95 (1995) 69.
[18] T. Saeki, K. Hashimoto, A. Fujishima, N. Kimura, K. Omata, The Journal of Physical Chemistry 99 (1995) 8440.
[19] T. Saeki, K. Hashimoto, N. Kimura, K. Omata, A. Fujishima, Chemistry Letters 5 (1995) 361.
[20] N. Ulagappan, H. Frei, Journal of Physical Chemistry A 104 (2000) 7834.
[21] N. Helaīli, Y. Bessekhouad, A. Bouguelia, M. Trari, Journal of Hazardous Materials 168 (2009) 484.
[22] S.C. Roy, O.K. Varghese, M. Paulose, C.A. Grimes, Acs Nano 4 (2010) 1259.
[23] P. Usubharatana, D. McMartin, A. Veawab, P. Tontiwachwuthikul, Journal of Industrial and Engineering Chemical Research 45 (2006) 2558.
[24] X.N. Wu, W.W. Weare, H. Frei, Dalton Transactions 45 (2009) 10114.
[25] S. Pradhan, D. Ghosh, S.W. Chen, Acs Applied Materials and Interfaces 1 (2009) 2060.
[26] M. Chung, D. Moon, K. Park, S. Ihm, Journal of Catalysis 136 (1992) 609.